Photochemical degradation of 4-nitrocatechol and 2,4-dinitrophenol in a sugar-glass secondary organic aerosol surrogate

*Avery B. Dalton, Sergey A. Nizkorodov**

Department of Chemistry, University of California, Irvine, Irvine, CA 92697

Abstract

The roles that chemical environment and viscosity play in the photochemical fate of molecules trapped in atmospheric particles are poorly understood. The goal of this work was to characterize the photolysis of 4-nitrocatechol (4NC) and 2,4-dinitrophenol (24DNP) in semi-solid isomalt as a new type of surrogate for glassy organic aerosol, and compare it to photolysis in liquid water, isopropanol, and octanol. UV/Vis spectroscopy was used to monitor the absorbance decay to determine the rates of photochemical loss of 4NC and 24DNP. The quantum yield of 4NC photolysis was found to be smaller in an isomalt glass (2.6×10^{-6}) than in liquid isopropanol (1.1×10^{-5}). Both 4NC and 24NDP had much lower photolysis rates in water than in organic matrices suggesting that they would photolyze more efficiently in organic aerosol particles than in cloud or fog droplets. Liquid chromatography in tandem with mass spectrometry was used to examine photolysis products of 4NC. In isopropanol solution, most products appeared to result from oxidation of 4NC, in stark contrast to photoreduction and dimerization products which were observed in solid isomalt. Therefore, the photochemical fate of 4NC, and presumably of other nitrophenols, should depend on whether they undergo photodegradation in a liquid or semi-solid organic particle.

Keywords

Condensed-phase photolysis, nitroaromatics, secondary organic aerosol proxy, glassy particles

Synopsis

Nitroaromatic compounds are more photochemically active in organic aerosol particles than in cloud droplets even if the particles are highly viscous.

Introduction

Secondary organic aerosol (SOA) is a complex mixture of different organic molecules, which can have a wide range of properties depending on SOA formation mechanisms and environmental

conditions. While SOA includes both gaseous and condensed-phase compounds, the term SOA is frequently used to refer only to the condensed phase, and we will follow the same convention in this paper. Models predict that the viscosity of SOA spans several orders of magnitude over a relatively small temperature range.[1] Both field measurements and laboratory studies have suggested that SOA exists as a viscous semi-solid or an amorphous glassy solid under low relative humidity and/or low temperature conditions, raising important questions about the effects of viscosity on atmospheric chemistry.[2-6] Viscosity has been shown to influence processes such as gas-particle partitioning, particle growth, the dynamics of coalescence of particles, and diffusion of molecules through SOA particles.[7-16] Since condensed-phase photochemical processes often include diffusion and secondary reactions of the photochemical reaction intermediates, the rate of photochemical processes in particles may also depend on viscosity. Though there have been recent studies investigating the effects of SOA viscosity on the photochemistry of select organic molecules, detailed characterization of photodegradation pathways of organic molecules in SOA has remained difficult due to the complex nature of the SOA material.[17,18]

The first goal of this work is to investigate the photochemistry of 4-nitrocatechol (4NC) under conditions representative of glassy SOA, to determine the rate of photochemical loss and propose products from photolysis. For comparison purposes, we also revisit the photochemistry of 2,4-dinitrophenol (24DNP) that previously examined in water and in organic solvents.[17-19] 4NC is an important component in light-absorbing brown carbon.[20-24] Both primary and secondary biomass burning organic aerosol (BBOA) have been found to contain 4NC, with a strong winter-time correlation to levoglucosan.[25] Secondary sources are thought to be more prevalent in the summer, formed via reactions of lignin pyrolysis products with NO_2.[25] Field studies have shown that 4NC is especially prevalent in BBOA, mostly close to the combustion source.[26-32] 24DNP is also commonly observed in ambient particles, alongside 4NC.[33] Laboratory studies have also shown that 4NC, 24DNP and related nitrophenols and nitrocatechols represent an important component in SOA generated through oxidation of aromatic compounds by NO_3 radicals or by OH in presence of NO_x.[34,35]

Previous studies of 4NC photochemistry focused on its behavior in gaseous phase and in aqueous solutions. Work by Zhao et al. looked at the pH dependence of 4NC aqueous phase photolysis by simulated sunlight and found the rate of photolysis to be quicker in a more acidic environment.[36]

The photolysis rate was measured by quantifying the rate of photoenhancement at 420 nm. These experiments also looked at the effects of adding an OH scavenger, with results supporting the notion that photochemical loss of 4NC happens through photolysis. Hems & Abbatt investigated the aqueous photooxidation of 4NC and other nitrophenols by OH, produced by photolysis of hydrogen peroxide.[37] In presence of OH, an initial increase in light-absorption by the solution was observed, with bleaching occurring over longer periods of time. This eventual decrease in color was not observed by photolysis alone (i.e., without the source of OH). These results have been attributed to an initial functionalization of 4NC by addition of OH followed by ring-opening and fragmentation, with the latter leading to the decrease in visible absorbance. While these authors concluded that direct photolysis is slower than OH oxidation under aqueous conditions, this conclusion cannot be generalized to conditions found in a highly viscous organic particle, where OH reactivity is expected to be limited to the surface.[38]

Photolysis of 24DNP was previously examined, and found to be much slower in water (polychromatic quantum yield of 8.1×10^{-5}) compared to organic solvents (polychromatic quantum yield of 2×10^{-3} in octanol).[17,19] The photolysis rate of 24DNP was found to be suppressed by increasing the viscosity of the organic matrix.[17] In contrast to 24DNP, the viscosity effects on photochemistry of 4NC have not been examined yet, which represents an important gap in knowledge considering that the atmospheric abundance of 4NC is higher than that of 24DNP.

When 4NC (or 24DNP) is trapped in an SOA particle, we expect the photoexcited 4NC to react predominantly with neighboring organic compounds via hydrogen abstraction. These reactions of nitrophenols can be classified as "indirect photolysis" since secondary reactions of the excited states generate the final products. In this paper we use a more general term "photodegradation" to encompass both direct and indirect photochemical processes occurring in the system. The hypothesized mechanism is shown in Reactions 1-3, where 4NC* represents a triplet excited state of 4NC (the short-lived singlet excited state is omitted for simplicity).

$$4NC + h\nu \rightarrow 4NC^* \qquad \text{Reaction 1}$$

$$4NC^* \rightarrow 4NC + \textit{heat} \qquad \text{Reaction 2}$$

$$4NC^* + R\text{-}H \rightarrow 4NC\text{-}H + R \qquad \text{Reaction 3}$$

$$4NC\text{-}H \rightarrow \textit{photoproducts} \qquad \text{Reaction 4}$$

Matrix viscosity is expected to play a role in Reaction 3 by limiting the diffusion of 4NC* to a reaction partner, an organic molecule with easily-abstractable hydrogen atoms. Examples include aldehydic hydrogen atoms, or hydrogen atoms attached to alpha-carbon atoms in alcohols, which can be stabilized in the carbon-centered radical (CCR) from of the hydrogen atom donor. We also expect that the R radical produced in Reaction 3 will go on to react and form various biproducts, making SOA composition even more complex.

The lifetime of 4NC* has not been reported in the literature, but the triplet state lifetimes in similar compounds like nitrophenols were observed to be less than one nanosecond.[39] On this short time scale, a highly viscous matrix could lead to a significant decrease in photoreactivity by hindering the ability of 4NC* to reorient itself for an optimal reaction with a suitable hydrogen atom donor. Viscosity could also play a role in the excited state dynamics leading to the formation of 4NC* by impacting the intersystem crossing efficiency from the excited singlet state to the triplet state.[40] Lignell et al. measured the effects of viscosity on the photochemistry of 24DNP, finding that a more viscous α-pinene SOA material led to stronger temperature and humidity dependence of the 24DNP photodegradation rate compared to less viscous octanol.[17] These were rather difficult experiments because of the small amount of SOA material – it is challenging to produce more than few hundred microgram of SOA with common aerosol science approaches.

In view of the experimental challenges of working with SOA material, the second goal of this work is to provide a convenient way to overcome the difficulty of photochemical experiments in viscous organic matrices by using a proxy organic material that resembles the physical and chemical properties of SOA. For this, we seek a semi-solid or glass organic matrix in which we can easily deposit a photolabile organic molecule of interest. Previous studies have considered octanol, citric acid, and sucrose as suitable candidates for organic aerosol mimics.[18,41-44] The use of sucrose as an SOA surrogate was motivated by findings that reported presence of carbohydrate-like molecules in ambient particles.[45,46] This work shows that isomaltitol (the structure of this sugar alcohol is shown in Fig. S1) can be used as an SOA surrogate that is in many ways superior to sucrose. Isomaltitol, commonly referred to as just isomalt, is predominately used as a sugar substitute in candies, baked goods, and pharmaceuticals.[47] Like sucrose, the functionality of isomalt is limited to hydroxyl groups, which is only one of the many types of functional groups present in SOA (such as carboxylic acids or aldehydes). However, this compound is exceedingly easy to work with since

it has relatively low glass transition and melting temperatures, 59°C and 142°C respectively,[48] and forms optically transparent glasses. Further, isomalt is thermally stable and does not decompose upon melting, unlike most other carbohydrates.[48] Isomalt is made up of an equimolar mixture of the diastereomers α-D-glucopyranosido-1,6-sorbitol and α-D-glucopyranosido-1,6-mannitol, a structure that has many abstractable hydrogen atoms resulting in stabilized CCR. These properties, combined with the expectation that isomalt will be photochemically inactive on its own, make isomalt a very convenient surrogate for experimental studies of photochemistry in glassy SOA.

Methods

Glass preparation

Isomalt glass was prepared by melting isomalt (food-grade, CK Products). In a beaker, ~7 g of isomalt were heated slowly on a hot plate. Initial experiments included a thermometer to monitor the temperature, but this was cumbersome due to the stickiness of the isomalt. It appeared to melt around 115°C. These initial experiments proved that keeping the hot plate set to low-medium heat was sufficient to keep the isomalt from burning. With these settings, the isomalt powder melted within 3-4 min. Isomalt that was overheated (>120°C) for long periods of time, approximately 5 min, would begin to turn yellow, and would eventually begin turning brown/black if burned.

The mass of isomalt was measured each time so that a sample volume could be estimated using the density of the glass. A measurement of the isomalt density was done by melting 2.50 grams of isomalt in a graduated cylinder, producing a volume of 1.54 mL upon solidification, giving a density of 1.62 g/cm^3. This is similar to the density of sucrose (1.6 g/cm^3), so in all calculations a density of 1.6 g/cm^3 was used.

A 210 μL aliquot of a 40 mM 4NC aqueous solution was added to the molten isomalt and was then swirled until the yellow color of 4NC was evenly distributed. The resulting concentration of 4NC in the glass was approximately 2 mM (millimoles of isomalt per 1000 cm^3 of glass). The 2 mM concentration was chosen to produce an absorbance of the order of one (transmittance of 0.1) at near-UV wavelengths. Given that typical glasses had a thickness around 1 mm, we aimed at a 4NC concentration that was ten times greater than an analogous experiment in a 1 cm cuvette would require.

The glass could only be formed reliably if the amount of water added to isomalt was < 500 µL. The formation of a glass seemed to be hindered by the addition of too much water, resulting in an isomalt slurry that failed to fully solidify. For example, the addition of 1-2 mL of water created glasses that would harden but retained air bubbles and appeared cloudy. The use of highly concentrated aqueous stock solutions allowed for spike volumes less than 500 µL which was a good threshold for maintaining an optically transparent glass. The spike volumes of 100-500 µL added to 9 g of isomalt worked well for glass preparation purposes (in all kinetics experiments 210 µL of 40 mM stock solution was used for consistency).

We also tried to add solid 4NC to isomalt before melting, thus eliminating water altogether, but this method was inferior compared to adding a solution of 4NC to molten isomalt as described above. When 4NC was added directly as a dry powder a low-viscosity yellow oil would form and would fail to homogeneously mix with the isomalt. There were minimal apparent issues with phase separation with adequately small additions of the stock solutions.

A drop of the molten isomalt/4NC mixture was poured onto a round fused silica window (Edmund Optics, 25 mm diameter, 2.3 mm thickness) and then immediately covered with a second window. The second window was held on the edges and pressed firmly by hand onto the molten glass, resulting in the glass cooling rapidly and solidifying. When being pressed, the isomalt glass would often form small fractures. To alleviate this issue, the sandwiched samples were heated directly on a hot plate until the fractures had fused together. This heating step also served to even out the thickness of the isomalt/4NC glass sample. The reheating was done for as short of a time as possible, less than a minute, to avoid overheating the isomalt. If left on the stove for too long, the sample would begin to bubble between the windows and pour off the sides. A reference for the UV/Vis was prepared by pouring pure molten isomalt without added 4NC onto a window and following the same procedure.

The same procedure outlined above was used to prepare 24DNP/isomalt samples, using a 350 µL aliquot of a 15 mM 24DNP (99.4%, Sigma Aldrich) aqueous solution to add to the molten isomalt.

Safety considerations

Preparation of isomalt glass requires the handling of hot glassware, the pouring of molten isomalt, and dealing with sharp isomalt glass. Heat-resistant gloves should be worn when handling

glassware containing molten isomalt. Care should be taken when pouring or mixing the molten isomalt, as contact with the skin can cause severe burns. Rapid cooling of isomalt can result in the formation of sharp edges and needle-like pieces. For this reason, avoid washing glassware containing isomalt glass by hand. We have found it simple to dispose of isomalt samples by carefully transferring the molten glass to a suitable heat-proof waste container.

Photolysis setup & product analysis

Experimental details about the UV/Vis and UPLC-PDA-HRMS used to conduct photolysis experiments and analyze products have been placed in the Supporting Information. Briefly, the sandwiched samples were photolyzed in a custom setup (Fig. S2) that continuously recorded UV/Vis transmission through the sample irradiated with broadband radiation in 290-500 nm range (Fig. S3). Photolysis in solution used the same light source that irradiated the solution in a cuvette inside a commercial UV/Vis spectrometer. Product analysis was conducted with a Thermo Scientific Vanquish Horizon ultra-performance liquid chromatograph (UPLC) in line with a Vanquish Horizon photodiode array (PDA) spectrometer and a Q Exactive Plus high-resolution mass spectrometer (HRMS).

Results and discussion

Molar extinction coefficient measurements

Experiments were conducted to quantify the molar extinction coefficients of 4NC in isopropanol and solid isomalt for comparison. Detailed results are reported in the Supporting Information section. The most important result of these measurements is that the spectrum of 4NC in isomalt shows a small (about 5 nm) bathochromic shift compared to isopropanol (Fig. S4). This makes it slightly more absorbing at the near-UV wavelengths that are responsible for driving photochemistry in the lower atmosphere. The peak molar extinction coefficient is essentially the same in isopropanol, $(7.1\pm0.2)\times10^3$ $M^{-1}cm^{-1}$ at 347 nm, and in solid isomalt, $(7.5\pm0.6)\times10^3$ $M^{-1}cm^{-1}$ at 350 nm (Fig. S5).

Photolysis kinetics

The rate of photochemical loss of 4NC and 24DNP was monitored by following the decay in absorbance of the glass or solution. An example of the absorption spectra recorded throughout

photolysis of 4NC in isomalt is presented in Fig. 1, and spectra of 4NC during photolysis in isopropanol are shown in Fig. S6. Figure 1 also shows the same spectra normalized to the initial absorbance at t=0 and the decay of this normalized absorbance at 370 nm.

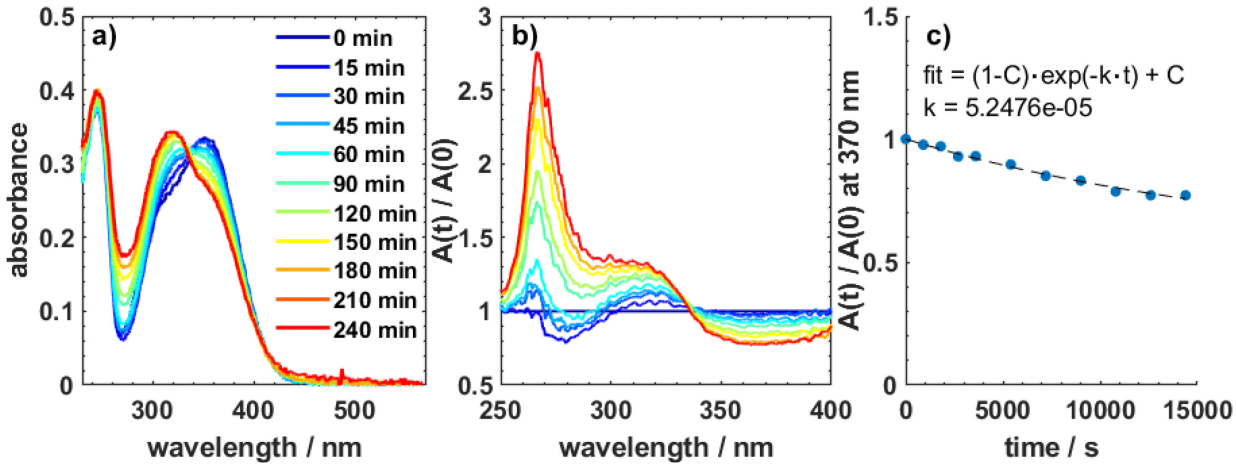

Figure 1. Plot of the absorption spectra of 4NC in isomalt glass obtained at different times during photolysis (a), the same absorbance spectra normalized to the absorbance at t = 0 (b), and the decay in normalized absorbance at 370 nm (c). Notable features of this data are the growth of absorbance at wavelengths below 340 nm and above 400 nm, as well as the decay around the 350 nm band of 4NC.

The normalized absorbance can be modelled by Equation 1.

$$\frac{A(t)}{A(0)} = \beta + (1 - \beta) \cdot \exp(-kt) \qquad \text{Equation 1}$$

which assumes that 4NC has a first-order decay forming a single product with a different absorption spectrum and no secondary photochemistry. The presence of the isosbestic point (near 340 nm in isomalt) in the data supports the assumption that only one product contributed to absorption in addition to 4NC (but does not exclude formation of additional weakly-absorbing products). The fitting parameter β represents the ratio of the molar extinction coefficient of the photolysis product to that of 4NC at the monitored wavelength and k is the first-order rate constant. Ideally, β should be zero at the observation wavelength but it is not achievable in practice. The wavelengths used for fitting the decay in the normalized absorbance were selected at point within the 4NC absorption peak that had the greatest decrease from the initial absorbance, where β should

have the smallest value. The chosen wavelengths varied between different matrices, with the largest decreases in absorbance occurring around 350 nm in isopropanol (Fig. S6) and octanol (Fig. S8) and around 370 nm in isomalt (Fig. 2(b)). For 24DNP (Fig. S9 & Fig. S10), the largest change was at 290 nm in octanol and 260 nm in isomalt.

On the timescale used in these experiments (3 to 5 h), we observed significant loss of 24DNP absorbance but absorbance of 4NC reduced by less than 30% (Fig. 1). Due to this, there was increased correlation between k and β, resulting in large uncertainties for k measured for 4NC (Table 1). Experiments were not conducted at longer timescales to avoid any secondary photochemistry of primary photolysis products. For short time scales, Equation 1 simplifies to Equation 2.

$$\frac{A(t)}{A(0)} = 1 - k\,(1-\beta)\,\mathrm{t} \qquad \text{Equation 2}$$

While the linear fit is more robust, it does not make it possible to determine k and β independently, and as such we report the product $k(1-\beta)$ in Table 1.The rate constants k from the exponential fit and $k(1-\beta)$ from the linear fit listed in Table 1 were similar in magnitude, hinting that β at the selected wavelengths was relatively small. In cases where β could be reliably obtained from the fit, the average fitted value of β at 350 nm obtained from three trials of 4NC in isomalt was ~0.014, whereas the fits in octanol and isopropanol yielded values of β around 10^{-6}. Therefore, in all cases, quantum yields were calculated from the more precise linear fit rate constants, assuming $\beta \approx 0$.

Table 1. Rate constants and quantum yields from photolysis of 4NC and 24DNP in various matrices

Molecule	**Matrix**	**k (s^{-1})[a] / 10^{-5}**	**k·(1-β) (s^{-1})[b] / 10^{-5}**	$\langle\phi\rangle$[c] / 10^{-5}	Lifetime in Los Angeles Atmosphere
4NC	Isomalt (**solid**)	5 ± 3[d]	1.8 ± 0.1	0.26 ± 0.02	24 d
-	Octanol (**film**)	3.2 ± 0.2	2.7 ± 0.1	0.40 ± 0.01	16 d
-	Isopropanol (**solution**)	5.4 ± 0.3	4.1 ± 0.2	1.07 ± 0.07	5.8 d
-	Water (**solution**)	0.09 ± 0.02	0.11 ± 0.03	0.013 ± 0.003	> 1 year

24DNP	Isomalt (**solid**)	2.9 ± 0.7	-[e]	36 ± 8	4 h
-	Octanol (**film**)	44 ± 3 20.4(1)[f]	-	180 ± 10 200[f]	1.2 h
-	SOM (**film**)	47.3(8)[f]	-	Not reported[f]	-
	Water (**solution**)			0.4[f] 8.1 ± 0.4[g]	

[a]The rate constant k is derived from the exponential decay in Equation 1. [b]The value of the slope from a linear fit that corresponds to the product $k(1 - \beta)$ from Equation 2. [c]Polychromatic quantum yield averaged over a 100 nm interval surrounding 350 nm for 4NC and 290 nm for 24DNP. [d]Error reported at a 95% confidence interval from the fits. [e]No linear fit was applied due to rapid decay of absorbance. [f]Secondary Organic Material (SOM) and octanol data from Lignell et al. 2014 measured at a different lamp power. [g]The quantum yield in water from Albinet et al. 2010.

Photolysis quantum yields

For optically thin samples, the first-order photolysis rate constant k can be related to the photolyzing radiation parameters as follows:

$$k = \int \phi(\lambda) \times \sigma(\lambda) \times F(\lambda)\, d\lambda \qquad \text{Equation 3}$$

The incident photons are represented by the spectral flux, $F(\lambda)$, shown in Fig. S3, and the wavelength-dependent molecular absorption cross section is $\sigma(\lambda)$. Since photolysis was done with a broadband light source, represented by the spectral flux density $F(\lambda)$, it is impossible to extract the wavelength dependence of the quantum yield from these data. An effective (polychromatic) quantum yield, $\langle\phi\rangle$ was determined by factoring it from the integral and integrating the remaining over a small wavelength range. In this work, the interval of integration was limited to 300-400 nm for 4NC, approximately 50 nm on either side of the main 350 nm peak in absorbance. Using the same logic for 24DNP, the interval 240-340 nm was used in octanol and isomalt. These intervals were used to encompass the main absorption bands of these molecules. Under this assumption, the effective quantum yield averaged over the wavelength integration range can be determined by the following equation.

$$\langle\phi\rangle = \frac{k}{\int \sigma(\lambda) \times F(\lambda)\, d\lambda} \qquad \text{Equation 4}$$

The polychromatic quantum yields are listed in Table 1. Results from triplicate experiments of 4NC photolysis in isomalt are shown in Table S1. The isomalt matrix appears to have good reproducibility in the photolysis experiments, which is an important factor for using as a surrogate for SOA photochemical studies.

Matrix effects on the 4NC and 24DNP photodegradation

Table 1 shows that rate constants varied depending on the local environment. For photolysis of 4NC, the reaction was the slowest in an aqueous environment $\langle\phi\rangle = 1.3\times10^{-7}$ and proceeded faster in solid isomalt (2.6×10^{-6}) and even faster in liquid octanol (4×10^{-6}) and isopropanol (1.1×10^{-5}). With the drastic difference between organic matrices and water, it is possible that while also being less reactive, water is more effective at quenching excited 4NC* (Reaction 2). Although the photochemical degradation in the organic solvents was slower in the isomalt glass than in liquid alcohols, it was still significantly quicker than in water. Despite the glassy nature of isomalt, photochemistry was not fully suppressed inside the isomalt matrix.

To put these results in perspective, we compare the measured quantum yields to a previous study by Lignell et. al (2014), who conducted experiments with 24DNP in both octanol and α-pinene secondary organic material (SOM).[17] Within experimental uncertainties, we obtained the same polychromatic quantum yield in octanol (1.8×10^{-3}) as Lignell et al. (2×10^{-3}). Our quantum yield of 24DNP in isomalt (3.6×10^{-4}) was lower than that in octanol. Although quantum yields were not reported for 24DNP in SOM by Lignell et al., their photolysis rate in SOM was twice of the rate in octanol. Since our observed quantum yields in isomalt and octanol followed the opposite trend, we predict that the glassy isomalt matrix is less reactive than α-pinene SOM in terms of reactivity with the triplet state of 24DNP. We will verify this prediction in future measurements.

Using the experimentally determined quantum yields, we estimated photochemical lifetimes of 4NC and 24DNP in the Los Angeles atmosphere from the reciprocal of the calculated rate constants from Equation 3. The 24-hour average spectral flux density, $F(\lambda)$, for Los Angeles, California (34° N, 118° W) on 20 June 2017 was simulated using the National Center for Atmospheric Research (NCAR) Tropospheric Ultraviolet and Visible (TUV) calculator. The photolysis lifetimes for 4NC in octanol and isomalt were found to be 16 and 24 days, respectively.

These fall within the range of the lifetimes of the overall brown carbon absorption coefficient of BBOA, reported as 10-41 days by Fleming et al. (2020).[22] However, in their work, they found the photochemical lifetime of 4NC in chamise fire BBOA to be ~12 hours, which they regarded as a lower limit. The slower photolysis of 4NC in octanol and isomalt glass suggest that organic molecules found in BBOA are even more efficient in reacting with triplet state of 4NC than alcohols are.

The lifetimes of 4NC with respect to OH oxidation have been evaluated by Hems & Abbatt.[37] In the aqueous phase the lifetime was measured to be 4.7 h, assuming [OH] = 1×10^{-14} M, and in the gaseous phase it was estimated to be 88 h (3.7 days), assuming [OH] = 1×10^{6} cm^{-3}. With the slow photolysis rate of 4NC in water, photolysis is not competitive with OH oxidation in the aqueous phase. However, photolysis in the organic phase occurs at a more comparable rate to gaseous OH oxidation. Therefore, the loss of 4NC could be controlled by photolysis when it is trapped in a highly viscous organic particle. The photolysis lifetimes for 24DNP are considerably shorter, 1.2 hours in octanol and 4 hours in isomalt under Los Angeles summer conditions. Considering that 24DNP is less volatile than 4NC, and therefore more likely to partition in particles, the photolysis of 24DNP in organic particles should be an important, and possibly the dominant loss mechanism for this molecule.

Photoproduct analysis

Total ion current (TIC) chromatograms produced from samples from before and after photolysis in both the isopropanol and the isomalt samples are shown in Figure 2. Figures S7 and S11 show select PDA absorption spectra of the products for photolysis in isopropanol and isomalt.

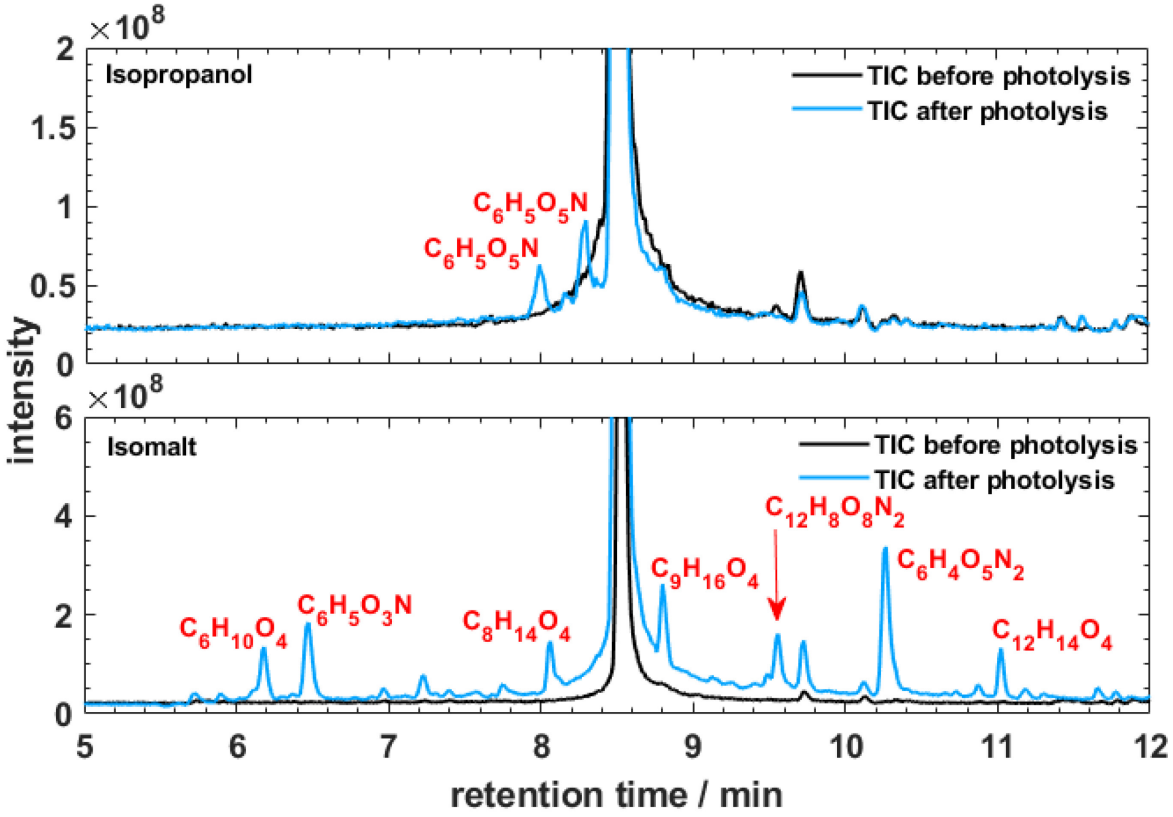

Figure 2. Total ion chromatograms from UPLC-HRMS analysis 4-nitrocatechol/isomalt glass samples before and after photolysis. Molecular formula assignments are provisional and represent the molecular species eluted at that peak retention time.

A summary of the observed photoproducts suggested by UPLC-PDA-HRMS analysis of 4NC photolysis samples is presented in Figure 3. We have observed different sets of products in the liquid and solid matrices. In solution, the primary photoproducts observed appear to correspond to an addition of -OH to 4NC ($C_6H_5O_4N \rightarrow C_6H_5O_5N$). It is important to note that experiments in isopropanol were open to the air, making it impossible to tell if the -OH was from the isopropanol solvent. Exposure to oxygen could have influenced formation of these oxidation products, through singlet oxygen formation or HO_x generated by the 4NC-H.[49,50]4NC has three distinct hydrogen atoms in the aromatic ring but both isopropanol and isomalt aqueous solutions had only two peaks for $C_6H_5O_5N$, suggesting two of three possible isomers are formed from this reaction. Due to a lack of analytical standards of these compounds, the preferred isomers could not be confirmed. The UV/Vis absorption spectra corresponding to these $C_6H_5O_5N$ products are shown in Figure S7.

The earlier eluted peak for this mass has a peak absorbance at 345 nm, while the spectrum of the later peak shows two maxima, one at 325 nm and one at 400 nm. It is possible that all three isomers of the -OH addition to 4NC are being formed but is impossible to confirm with a lack of published absorption spectra for two of the three isomers.

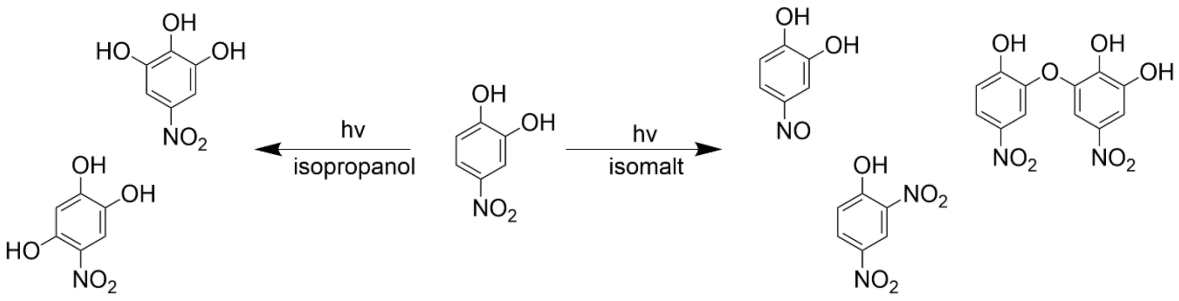

Figure 3. Products formed during photolysis of 4-nitrocatechol in an isopropanol solution (left) and an amorphous isomalt glass (right). The structural assignments presented should be considered provisional.

In contrast to experiments in solution, 4NC embedded in isomalt appears to have formed some dimers of 4NC. Although the melted isomalt/4NC mixture appeared as one phase, it is possible that 4NC were forming complexes together in the matrix promoted by π-π stacking interactions (this would be consistent with the observed small bathochromic shift in isomalt, Fig. S4). The proximity between two 4NC molecules would promote 4NC*+4NC reaction instead of 4NC*+isomalt reaction, as the H atoms on the hydroxyl groups in catechols are also easily abstractable. Signal for 4NC dimers in the non-photolyzed candy was very low, so it is unlikely that heating caused excessive dimerization. It has been reported that inside of a viscous organic particle, diffusion of oxygen into the particle is minimal, giving rise to persistent radicals and allowing for radical recombination between neighboring 4NC-H.[41]

The isomalt matrix appears to have also yielded the oxygen loss product ($C_6H_5O_4N \rightarrow C_6H_5O_3N$), which could be the replacement of -OH with -H or the loss of an -O from the NO_2 group. The PDA UV/Vis spectrum had a pronounced peak at 322 nm shown in Fig. S11(C). A peak at this absorbance is not characteristic 2-nitrophenol in aqueous solution.[42,51] A study of aqueous 4-nitrophenol photolysis showed an absorbance maximum at 325 nm, which is relatively close.[51,52]

However, we only observed a single isomer of $C_6H_5O_3N$ in single ion chromatograms, which is an argument against assigning this product to 4-nitrophenol. Absorption spectra of 4-nitrosocatechol could not be found in the literature. The absorption spectrum for 4-nitrosophenol has been reported with a maximum around 300 nm.[53] If the additional OH group causes the same red-shift in absorption between 4-nitrosophenol and 4-nitrosocatechol as it shows between phenol and catechol, it is likely that 4-nitrosocatechol is being observed.[54,55] Furthermore, the fragmentation spectrum of the ion corresponding to $C_6H_5O_3N$ (Fig. S12) contained a peak corresponding to the loss of NO, but no peak corresponding to the loss of NO_2. Therefore, we assigned the photoproduct observed here to 4-nitrosocatechol, as indicated in Fig. 3. Nitroso compounds are highly reactive, so 4-nitrosocatechol is likely to proceed to secondary products.

24DNP was also observed as a product unique to photolysis of 4NC in isomalt ($C_6H_5O_4N \rightarrow C_6H_4O_5N_2$). A single peak was eluted for $C_6H_4O_5N_2$ with a corresponding PDA UV/Vis spectrum that peaks at 260 and 290 nm (Fig S11(G)). This product is somewhat unexpected, as it would require a direct swap of -OH for -NO_2. If this replacement happened in two steps, we would expect to also observe products corresponding to loss of -OH. As previously discussed, loss of -OH was not evident. Further, for 24DNP to be the product the -OH loss product would have needed to be 2-nitrophenol, which was ruled out based on the UV/Vis spectrum. If 24DNP is being formed as a product of 4NC photolysis, it seems most likely that it is occurring in a direct 4NC*+4NC reaction.

Finally, the chromatogram contained peaks that could not reasonably come from 4NC, for example, peaks corresponding to neutral formulas $C_6H_{10}O_4$, $C_8H_{14}O_4$, $C_9H_{16}O_4$, and $C_{12}H_{14}O_4$. Hydrolysis of isomalt would yield glucose, mannitol, and sorbitol (all $C_6H_{12}O_6$), which none of the observed formulas correspond to. Dehydration of the glucose, mannitol, or sorbitol components of isomalt does not explain observation of $C_6H_{10}O_4$. The $C_6H_{12}O_6 \rightarrow C_6H_{10}O_4$ transformation would require loss of H_2O_2. This implies that the photoreduction of 4NC could lead to peroxide formation in the isomalt matrix, similar to how irradiation of nitro-polycyclic aromatic hydrocarbons has been shown to lead to peroxide formation in methyl lineolate.[56] Oxygen could have potentially entered the matrix as air bubbles during sample preparation. Although oxygen is expected to be depleted quickly by free radicals, a small portion would have been available for reaction.[57] The mechanistic details of this process will be explored in future studies.

Atmospheric Implications

This work uses isomalt as a proxy for a glassy SOA matrix. The use of isomalt provides a simple preparation of a photolysis medium that, by itself, is optically transparent and photochemically stable. Our experiments on photochemistry of 4NC and 24DNP show that candy-like isomalt is a convenient matrix for reproducible photochemical experiments and product analysis. This simple method opens new avenues for atmospheric condensed-phase photochemical experiments, not only on nitrophenols, but on other photochemically active organic compounds.

We observe that photodegradation rates of 4NC and 24DNP in solid isomalt are comparable to those in liquid octanol and isopropanol. This is an important result demonstrating that photochemistry of nitrophenols can occur even when they are trapped in a highly viscous organic particles. The estimated photochemical lifetimes of 4NC in the organic phase are comparable to those of OH oxidation in the gas phase. For 24DNP, the major loss mechanism will be dependent on the viscosity of the organic particle it is trapped in.

The different types of products for 4NC photolysis in isopropanol and isomalt represent another important result of this work. In isopropanol, only products corresponding to the addition of -OH groups are observed. In contrast, photolysis in isomalt glass results in 4NC dimerization, and formation of products corresponding to an addition of $-NO_2$, or loss of -OH from 4NC. There is evidence of photoreduction of 4NC, which is an uncommon process for the highly oxidizing atmospheric environment, and produces highly-reactive nitroso compounds. Varying photoproducts between the solid and liquid environment have implications for understanding the environmental fates of nitrophenols, with products being dependent on the specific environment nitrophenols are exposed to during their atmospheric transport.

AUTHOR INFORMATION

Corresponding Author

* E-mail: nizkorod@uci.edu

ORCID

Avery B. Dalton: 0000-0002-6923-9090

Sergey A. Nizkorodov: 0000-0003-0891-0052

Author Contributions

The experiments and data analysis were conceived by ABD and SAN, and carried out by ABD. The manuscript was written by ABD and edited by SAN. Both authors have approved the final version of the manuscript.

Notes

The authors declare no competing financial interest.

Supporting Information

Method description has been placed in the Supporting Information, along with figures from the more detailed analyses. They include structures of the chemicals used (Fig. S1), schematic of the solid-state photolysis setup (Fig. S2), spectrum of the irradiation source (Fig. S3), molar extinction coefficient measurement results (Figs. S4 and S5), results for photolysis in isopropanol solution (Figs. S6 and S7), octanol film (Figs. S8 and S9), and solid isomalt (Figs. S10, S11, S12 and Table S1).

Acknowledgements

This work was supported by the US National Science Foundation grant AGS-1853639. The high-resolution mass spectrometer instrument used in this work was purchased with the US National Science Foundation grant CHE-1920242. The authors thank Natalie R. Smith for help with using the high-resolution mass spectrometer.

References

(1) Gervasi, N. R.; Topping, D. O.; Zuend, A. A Predictive Group-Contribution Model for the Viscosity of Aqueous Organic Aerosol. *Atmospheric Chemistry and Physics* **2020**, *20* (5), 2987–3008.

(2) Reid, J. P.; Bertram, A. K.; Topping, D. O.; Laskin, A.; Martin, S. T.; Petters, M. D.; Pope, F. D.; Rovelli, G. The Viscosity of Atmospherically Relevant Organic Particles. *Nature Communications* **2018**, *9* (1), 956.

(3) Bateman, A. P.; Bertram, A. K.; Martin, S. T. Hygroscopic Influence on the Semisolid-to-Liquid Transition of Secondary Organic Materials. *J. Phys. Chem. A* **2015**, *119* (19), 4386–4395.

(4) Renbaum-Wolff, L.; Grayson, J. W.; Bateman, A. P.; Kuwata, M.; Sellier, M.; Murray, B. J.; Shilling, J. E.; Martin, S. T.; Bertram, A. K. Viscosity of α-Pinene Secondary Organic Material and Implications for Particle Growth and Reactivity. *PNAS* **2013**, *110* (20), 8014–8019.

(5) Koop, T.; Bookhold, J.; Shiraiwa, M.; Pöschl, U. Glass Transition and Phase State of Organic Compounds: Dependency on Molecular Properties and Implications for Secondary Organic Aerosols in the Atmosphere. *Phys. Chem. Chem. Phys.* **2011**, *13* (43), 19238–19255.

(6) Kidd, C.; Perraud, V.; Wingen, L. M.; Finlayson-Pitts, B. J. Integrating Phase and Composition of Secondary Organic Aerosol from the Ozonolysis of α-Pinene. *PNAS* **2014**, *111* (21), 7552–7557.

(7) Maclean, A. M.; Smith, N. R.; Li, Y.; Huang, Y.; Hettiyadura, A. P. S.; Crescenzo, G. V.; Shiraiwa, M.; Laskin, A.; Nizkorodov, S. A.; Bertram, A. K. Humidity-Dependent Viscosity of Secondary Organic Aerosol from Ozonolysis of β-Caryophyllene: Measurements, Predictions, and Implications. *ACS Earth Space Chem.* **2021**, *5* (2), 305–318.

(8) Zaveri, R. A.; Shilling, J. E.; Zelenyuk, A.; Liu, J.; Bell, D. M.; D'Ambro, E. L.; Gaston, C. J.; Thornton, J. A.; Laskin, A.; Lin, P.; Wilson, J.; Easter, R. C.; Wang, J.; Bertram, A. K.; Martin, S. T.; Seinfeld, J. H.; Worsnop, D. R. Growth Kinetics and Size Distribution Dynamics of Viscous Secondary Organic Aerosol. *Environ. Sci. Technol.* **2018**, *52* (3), 1191–1199.

(9) Wang, B.; O'Brien, R. E.; Kelly, S. T.; Shilling, J. E.; Moffet, R. C.; Gilles, M. K.; Laskin, A. Reactivity of Liquid and Semisolid Secondary Organic Carbon with Chloride and Nitrate in Atmospheric Aerosols. *J. Phys. Chem. A* **2015**, *119* (19), 4498–4508.

(10) Shiraiwa, M.; Ammann, M.; Koop, T.; Pöschl, U. Gas Uptake and Chemical Aging of Semisolid Organic Aerosol Particles. *PNAS* **2011**, *108* (27), 11003–11008.

(11) Power, R. M.; Simpson, S. H.; Reid, J. P.; Hudson, A. J. The Transition from Liquid to Solid-like Behaviour in Ultrahigh Viscosity Aerosol Particles. *Chem. Sci.* **2013**, *4* (6), 2597–2604.

(12) Rothfuss, N. E.; Petters, M. D. Coalescence-Based Assessment of Aerosol Phase State Using Dimers Prepared through a Dual-Differential Mobility Analyzer Technique. *Aerosol Science and Technology* **2016**, *50* (12), 1294–1305.

(13) Vaden, T. D.; Imre, D.; Beránek, J.; Shrivastava, M.; Zelenyuk, A. Evaporation Kinetics and Phase of Laboratory and Ambient Secondary Organic Aerosol. *PNAS* **2011**, *108* (6), 2190–2195.

(14) Perraud, V.; Bruns, E. A.; Ezell, M. J.; Johnson, S. N.; Yu, Y.; Alexander, M. L.; Zelenyuk, A.; Imre, D.; Chang, W. L.; Dabdub, D.; Pankow, J. F.; Finlayson-Pitts, B. J. Nonequilibrium Atmospheric Secondary Organic Aerosol Formation and Growth. *PNAS* **2012**, *109* (8), 2836–2841.

(15) Wall, A. C. V.; Perraud, V.; M. Wingen, L.; J. Finlayson-Pitts, B. Evidence for a Kinetically Controlled Burying Mechanism for Growth of High Viscosity Secondary Organic Aerosol. *Environmental Science: Processes & Impacts* **2020**, *22* (1), 66–83.

(16) Yli-Juuti, T.; Pajunoja, A.; Tikkanen, O.-P.; Buchholz, A.; Faiola, C.; Väisänen, O.; Hao, L.; Kari, E.; Peräkylä, O.; Garmash, O.; Shiraiwa, M.; Ehn, M.; Lehtinen, K.; Virtanen, A. Factors Controlling the

Evaporation of Secondary Organic Aerosol from α-Pinene Ozonolysis. *Geophysical Research Letters* **2017**, *44* (5), 2562–2570.

(17) Lignell, H.; Hinks, M. L.; Nizkorodov, S. A. Exploring Matrix Effects on Photochemistry of Organic Aerosols. *PNAS* **2014**, *111* (38), 13780–13785.

(18) Hinks, M. L.; Brady, M. V.; Lignell, H.; Song, M.; Grayson, J. W.; Bertram, A. K.; Lin, P.; Laskin, A.; Laskin, J.; Nizkorodov, S. A. Effect of Viscosity on Photodegradation Rates in Complex Secondary Organic Aerosol Materials. *Phys. Chem. Chem. Phys.* **2016**, *18* (13), 8785–8793.

(19) Albinet, A.; Minero, C.; Vione, D. Phototransformation Processes of 2,4-Dinitrophenol, Relevant to Atmospheric Water Droplets. *Chemosphere* **2010**, *80* (7), 753–758.

(20) Bluvshtein, N.; Lin, P.; Flores, J. M.; Segev, L.; Mazar, Y.; Tas, E.; Snider, G.; Weagle, C.; Brown, S. S.; Laskin, A.; Rudich, Y. Broadband Optical Properties of Biomass-Burning Aerosol and Identification of Brown Carbon Chromophores. *Journal of Geophysical Research: Atmospheres* **2017**, *122* (10), 5441–5456.

(21) Caumo, S. E. S.; Claeys, M.; Maenhaut, W.; Vermeylen, R.; Behrouzi, S.; Safi Shalamzari, M.; Vasconcellos, P. C. Physicochemical Characterization of Winter PM10 Aerosol Impacted by Sugarcane Burning from São Paulo City, Brazil. *Atmospheric Environment* **2016**, *145*, 272–279.

(22) Fleming, L. T.; Lin, P.; Roberts, J. M.; Selimovic, V.; Yokelson, R.; Laskin, J.; Laskin, A.; Nizkorodov, S. A. Molecular Composition and Photochemical Lifetimes of Brown Carbon Chromophores in Biomass Burning Organic Aerosol. *Atmospheric Chemistry and Physics* **2020**, *20* (2), 1105–1129.

(23) Kahnt, A.; Behrouzi, S.; Vermeylen, R.; Safi Shalamzari, M.; Vercauteren, J.; Roekens, E.; Claeys, M.; Maenhaut, W. One-Year Study of Nitro-Organic Compounds and Their Relation to Wood Burning in PM10 Aerosol from a Rural Site in Belgium. *Atmospheric Environment* **2013**, *81*, 561–568.

(24) Xie, M.; Chen, X.; Hays, M. D.; Holder, A. L. Composition and Light Absorption of N-Containing Aromatic Compounds in Organic Aerosols from Laboratory Biomass Burning. *Atmospheric Chemistry and Physics* **2019**, *19* (5), 2899–2915.

(25) Al-Naiema, I. M.; Offenberg, J. H.; Madler, C. J.; Lewandowski, M.; Kettler, J.; Fang, T.; Stone, E. A. Secondary Organic Aerosols from Aromatic Hydrocarbons and Their Contribution to Fine Particulate Matter in Atlanta, Georgia. *Atmospheric Environment* **2020**, *223*, 117227.

(26) Iinuma, Y.; Brüggemann, E.; Gnauk, T.; Müller, K.; Andreae, M. O.; Helas, G.; Parmar, R.; Herrmann, H. Source Characterization of Biomass Burning Particles: The Combustion of Selected European Conifers, African Hardwood, Savanna Grass, and German and Indonesian Peat. *Journal of Geophysical Research: Atmospheres* **2007**, *112* (D8), D08209, doi:10.1029/2006JD007120.

(27) Iinuma, Y.; Keywood, M.; Herrmann, H. Characterization of Primary and Secondary Organic Aerosols in Melbourne Airshed: The Influence of Biogenic Emissions, Wood Smoke and Bushfires. *Atmospheric Environment* **2016**, *130*, 54–63.

(28) Bertrand, A.; Stefenelli, G.; Jen, C. N.; Pieber, S. M.; Bruns, E. A.; Ni, H.; Temime-Roussel, B.; Slowik, J. G.; Goldstein, A. H.; El Haddad, I.; Baltensperger, U.; Prévôt, A. S. H.; Wortham, H.;

Marchand, N. Evolution of the Chemical Fingerprint of Biomass Burning Organic Aerosol during Aging. *Atmos. Chem. Phys.* **2018**, *18* (10), 7607–7624.

(29) Bluvshtein, N.; Lin, P.; Flores, J. M.; Segev, L.; Mazar, Y.; Tas, E.; Snider, G.; Weagle, C.; Brown, S. S.; Laskin, A.; Rudich, Y. Broadband Optical Properties of Biomass-Burning Aerosol and Identification of Brown Carbon Chromophores. *Journal of Geophysical Research: Atmospheres* **2017**, *122* (10), 5441–5456.

(30) Lin, P.; Aiona, P. K.; Li, Y.; Shiraiwa, M.; Laskin, J.; Nizkorodov, S. A.; Laskin, A. Molecular Characterization of Brown Carbon in Biomass Burning Aerosol Particles. *Environ. Sci. Technol.* **2016**, *50* (21), 11815–11824

(31) Lin, P.; Bluvshtein, N.; Rudich, Y.; Nizkorodov, S. A.; Laskin, J.; Laskin, A. Molecular Chemistry of Atmospheric Brown Carbon Inferred from a Nationwide Biomass Burning Event. *Environ. Sci. Technol.* **2017**, *51* (20), 11561–11570.

(32) Yuan, W.; Huang, R.-J.; Yang, L.; Wang, T.; Duan, J.; Guo, J.; Ni, H.; Chen, Y.; Chen, Q.; Li, Y.; Dusek, U.; O'Dowd, C.; Hoffmann, T. Measurement Report: $PM_{2.5}$-Bound Nitrated Aromatic Compounds in Xi'an, Northwest China – Seasonal Variations and Contributions to Optical Properties of Brown Carbon. *Atmospheric Chemistry and Physics* **2021**, *21* (5), 3685–3697.

(33) Harrison, M. A. J.; Barra, S.; Borghesi, D.; Vione, D.; Arsene, C.; Iulian Olariu, R. Nitrated Phenols in the Atmosphere: A Review. *Atmospheric Environment* **2005**, *39* (2), 231–248.

(34) Finewax, Z.; de Gouw, J. A.; Ziemann, P. J. Identification and Quantification of 4-Nitrocatechol Formed from OH and NO_3 Radical-Initiated Reactions of Catechol in Air in the Presence of NO_x: Implications for Secondary Organic Aerosol Formation from Biomass Burning. *Environ. Sci. Technol.* **2018**, *52* (4), 1981–1989.

(35) Lin, P.; Liu, J.; Shilling, J. E.; Kathmann, S. M.; Laskin, J.; Laskin, A. Molecular Characterization of Brown Carbon (BrC) Chromophores in Secondary Organic Aerosol Generated from Photo-Oxidation of Toluene. *Phys. Chem. Chem. Phys.* **2015**, *17* (36), 23312–23325.

(36) Zhao, R.; Lee, A. K. Y.; Huang, L.; Li, X.; Yang, F.; Abbatt, J. P. D. Photochemical Processing of Aqueous Atmospheric Brown Carbon. *Atmospheric Chemistry and Physics* **2015**, *15* (11), 6087–6100.

(37) Hems, R. F.; Abbatt, J. P. D. Aqueous Phase Photo-Oxidation of Brown Carbon Nitrophenols: Reaction Kinetics, Mechanism, and Evolution of Light Absorption. *ACS Earth Space Chem.* **2018**, *2* (3), 225–234.

(38) Bertram, A. K.; Ivanov, A. V.; Hunter, M.; Molina, L. T.; Molina, M. J. The Reaction Probability of OH on Organic Surfaces of Tropospheric Interest. *J. Phys. Chem. A* **2001**, *105* (41), 9415–9421.

(39) Takezaki, M.; Hirota, N.; Terazima, M. Nonradiative Relaxation Processes and Electronically Excited States of Nitrobenzene Studied by Picosecond Time-Resolved Transient Grating Method. *J. Phys. Chem. A* **1997**, *101* (19), 3443–3448.

(40) Nagarajan, K.; Mallia, A. R.; Muraleedharan, K.; Hariharan, M. Enhanced Intersystem Crossing in Core-Twisted Aromatics. *Chem. Sci.* **2017**, *8* (3), 1776–1782.

(41) Alpert, P. A.; Dou, J.; Corral Arroyo, P.; Schneider, F.; Xto, J.; Luo, B.; Peter, T.; Huthwelker, T.; Borca, C. N.; Henzler, K. D.; Schaefer, T.; Herrmann, H.; Raabe, J.; Watts, B.; Krieger, U. K.; Ammann, M. Photolytic Radical Persistence Due to Anoxia in Viscous Aerosol Particles. *Nat Commun* **2021**, *12* (1), 1769.

(42) Barsotti, F.; Bartels-Rausch, T.; De Laurentiis, E.; Ammann, M.; Brigante, M.; Mailhot, G.; Maurino, V.; Minero, C.; Vione, D. Photochemical Formation of Nitrite and Nitrous Acid (HONO) upon Irradiation of Nitrophenols in Aqueous Solution and in Viscous Secondary Organic Aerosol Proxy. *Environ. Sci. Technol.* **2017**, *51* (13), 7486–7495.

(43) Kiland, K. J.; Maclean, A. M.; Kamal, S.; Bertram, A. K. Diffusion of Organic Molecules as a Function of Temperature in a Sucrose Matrix (a Proxy for Secondary Organic Aerosol). *J. Phys. Chem. Lett.* **2019**, *10* (19), 5902–5908.

(44) H. Marshall, F.; Berkemeier, T.; Shiraiwa, M.; Nandy, L.; B. Ohm, P.; S. Dutcher, C.; P. Reid, J. Influence of Particle Viscosity on Mass Transfer and Heterogeneous Ozonolysis Kinetics in Aqueous–Sucrose–Maleic Acid Aerosol. *Physical Chemistry Chemical Physics* **2018**, *20* (22), 15560–15573.

(45) Russell, L. M.; Hawkins, L. N.; Frossard, A. A.; Quinn, P. K.; Bates, T. S. Carbohydrate-like Composition of Submicron Atmospheric Particles and Their Production from Ocean Bubble Bursting. *PNAS* **2010**, *107* (15), 6652–6657.

(46) Simoneit, B. R. T.; Elias, V. O.; Kobayashi, M.; Kawamura, K.; Rushdi, A. I.; Medeiros, P. M.; Rogge, W. F.; Didyk, B. M. Sugars Dominant Water-Soluble Organic Compounds in Soils and Characterization as Tracers in Atmospheric Particulate Matter. *Environ. Sci. Technol.* **2004**, *38* (22), 5939–5949.

(47) Sentko, A.; Willibald-Ettle, I. Isomalt. In *Sweeteners and Sugar Alternatives in Food Technology*; John Wiley & Sons, Ltd; pp 243–274.

(48) Cammenga, H. K.; Zielasko, B. Thermal Behaviour of Isomalt. *Thermochimica Acta* **1996**, *271*, 149–153.

(49) Ossola, R.; Jönsson, O. M.; Moor, K.; McNeill, K. Singlet Oxygen Quantum Yields in Environmental Waters. *Chem. Rev.* **2021**, *121* (7), 4100–4146.

(50) Corral Arroyo, P.; Bartels-Rausch, T.; Alpert, P. A.; Dumas, S.; Perrier, S.; George, C.; Ammann, M. Particle-Phase Photosensitized Radical Production and Aerosol Aging. *Environ. Sci. Technol.* **2018**, *52* (14), 7680–7688.

(51) Vione, D.; Maurino, V.; Minero, C.; Duncianu, M.; Olariu, R.-I.; Arsene, C.; Sarakha, M.; Mailhot, G. Assessing the Transformation Kinetics of 2- and 4-Nitrophenol in the Atmospheric Aqueous Phase. Implications for the Distribution of Both Nitroisomers in the Atmosphere. *Atmospheric Environment* **2009**, *43* (14), 2321–2327.

(52) Braman, T.; Dolvin, L.; Thrasher, C.; Yu, H.; Walhout, E. Q.; O'Brien, R. E. Fresh versus Photo-Recalcitrant Secondary Organic Aerosol: Effects of Organic Mixtures on Aqueous Photodegradation of 4-Nitrophenol. *Environ. Sci. Technol. Lett.* **2020**, *7* (4), 248–253.

(53) Lian, H.-Z.; Wei, Y.-N.; Liu, W.-W.; Li, D.-D. HPLC-UV Detection for Analysis of P-Benzoquinone Dioxime and P-Nitrosophenol, and Chromatographic Fingerprint Applied in Quality

Control of Industrial P-Benzoquinone Dioxime. *Journal of Liquid Chromatography & Related Technologies* **2006**, *29* (4), 509–520.

(54) Dewar, M. J. S.; Kubba, V. P.; Pettit, R. New Heteroaromatic Compounds. Part II. Boron Compounds Isoconjugate with Indole, 2:3-Benzofuran, and Thionaphthen. *J. Chem. Soc.* **1958**, 3076–3079.

(55) Martynoff, M. Note de Laboratoire: Spectres d'absorption de Quelques p-Quinones. *Bull. Soc. Chim. Fr.* **1949**, *16*, 258–261.

(56) Xia, Q.; Yin, J.-J.; Zhao, Y.; Wu, Y.-S.; Wang, Y.-Q.; Ma, L.; Chen, S.; Sun, X.; Fu, P. P.; Yu, H. UVA Photoirradiation of Nitro-Polycyclic Aromatic Hydrocarbons—Induction of Reactive Oxygen Species and Formation of Lipid Peroxides. *International Journal of Environmental Research and Public Health* **2013**, *10* (3), 1062–1084.

(57) Renard, P.; Reed Harris, A. E.; Rapf, R. J.; Ravier, S.; Demelas, C.; Coulomb, B.; Quivet, E.; Vaida, V.; Monod, A. Aqueous Phase Oligomerization of Methyl Vinyl Ketone by Atmospheric Radical Reactions. *J. Phys. Chem. C* **2014**, *118* (50), 29421–29430.

TOC graphic for manuscript: